

## Supplementary Data

### Neutrophil migration in Dunn Chamber Assay

To better understand the nature of the migratory defect, we performed real time imaging using a Dunn chamber, which allows direct visualization of neutrophil motility and directional migration along a chemokine gradient. Overall, a significantly lower percentage of *Srf* KO than WT neutrophils migrated towards the fMLP gradient (Suppl. Figure 3A; WT  $53.44 \pm 3.12\%$  vs. KO  $18.83 \pm 5.11\%$ ;  $p = 0.029$ ). In addition, *Srf* WT neutrophils migrated rapidly towards the fMLP gradient, while those *Srf* KO neutrophils that migrated (with cut-off of minimum distance of  $7.5\mu\text{m}$ ) achieved a significantly lower translocation distance (Suppl. Figure 3B; WT  $54.29 \pm 0.40 \mu\text{m}/30\text{min}$  vs. KO  $27.68 \pm 0.19 \mu\text{m}/30\text{min}$ ;  $p=0.0003$ ). Movies show WT (Video 1) and KO (Video 2) neutrophil migration. Thus *Srf* KO neutrophils have a severe migration defect *in vitro*, which is likely responsible for the lack of neutrophil accumulation at sites of inflammation *in vivo*.

### Cell adhesion is defective in *Srf* KO neutrophils

Integrins LFA1 and Mac1 play distinct roles in neutrophil adhesion. While LFA1 predominantly functions in the initial engagement of the neutrophil with the endothelium leading to rolling followed by arrest, binding of endothelial ICAM-1 to Mac-1 induces neutrophil crawling on the endothelial surface and transmigration through endothelial pores. We tested neutrophil adhesion in response to fMLP. Equal numbers of *Srf* WT and KO neutrophils were allowed to adhere to uncoated or fibrinogen-coated glass coverslips with or without stimulation with fMLP. Non-adherent neutrophils were removed by gentle rinsing. Significantly fewer *Srf* KO neutrophils adhered to uncoated or fibrinogen coated coverslips following stimulation with fMLP. Shown in Supplemental Figure 4.

## Supplementary Methods

### Dunn chamber assay

Equal numbers of WT and KO neutrophils were allowed to adhere to fibrinogen-coated coverslips, which were inverted onto a Dunn Chamber (Hawksley, Lancing, Sussex). Migration towards an fMLP gradient across the Dunn chamber bridge was imaged every 30 seconds over a period of 30 minutes. Images were analyzed using MetaMorph and Microsoft Excel Software as previously described.<sup>1</sup>

### Adhesion Assay

For cellular adhesion isolated neutrophils were stimulated with vehicle or fMLP and allowed to adhere to uncoated or fibrinogen-coated coverslips. Non-adherent cells were gently washed off. Adherent cells were counted on 5 20x fields and averaged. The experiment was repeated 3 times.

**Figure S1:** (A) Neutrophil morphology from *Srf* WT and KO mice. (B) White cell count (WBC) and white cell differential in primary Dox-inducible Cre *Srf* WT  $n=11$  and

KO n=10 mice. Peripheral blood from Dox-inducible Cre/*Srf* bone marrow transplanted mice aged 4 weeks was obtained after treatment with doxycycline for 8-10 days and WBC and WBC differential assessed on a Hemavet. *Srf* expression in Neutrophils from dox-inducible *Srf* WT and KO mice assessed by qRT-PCR (C) and Western blot (D).

**Figure S2:** Lung immunohistology of recipients of Dox-inducible *Srf* WT and KO bone marrow probed for the neutrophil specific antibody 7/4 prior to (0hr) and 4 (4hr) and 24 hours (24hr) after LPS nebulization (60x magnification; Size bar=20 $\mu$ m).

**Figure S3:** CXCR2 expression and migration of *Srf* WT and KO neutrophils in Dunn chamber assay. (A) CXCR2 expression was assessed by flow-cytometry on *Srf* WT and KO neutrophils. (B,C) *Srf* WT and KO neutrophils were directly imaged while exposed to fMLP gradient in a Dunn chamber. (B) The percentage of migrating neutrophils was assessed with a cut-off of 7.5 $\mu$ m, which corresponds to one-half the diameter of an activated neutrophil. (C) The translocation distance in  $\mu$ m was measured for those neutrophils, that migrated at least 7.5 $\mu$ m (\* $p$ <.05; \*\*\* $p$ <.0005).

**Figure S4:** Integrin Expression and Adhesion. Gene expression was assessed in *Srf* WT and KO neutrophils by qRT-PCR (A). CD11b and CD11a expression was assessed by flow-cytometry in *Srf* WT and KO neutrophils 0, 2, and 5 minutes after fMLP stimulation (B). *Srf* WT and KO neutrophils were allowed to adhere to untreated or fibrinogen coated glass coverslips in the absence or presence of activation with fMLP (C). Representative of 3 independent experiments, number of fields counted per slide (n)=5. (\*\* $p$ <.0005, \* $p$ <.05)

**Figure S5:** Immunofluorescence quantification. Quantification of cells from Figure 6. (A) Percent of cells with polarized CD11b; n = number of cells: WT 0 min. n=28, WT 15 min. n=32, KO 0 min. n=12, KO 15 min. n=12 cells. (B) Percent of cells with polarized clathrin; WT 0 min. n=25, WT 15 min. n=45, KO 0 min. n=24, KO 15 min. n=30 cells. (C) Percent of cells with polarized kindlin; WT 0 min. n=82, WT 15 min. n=151, KO 0 min. n=64, KO 15 min. n=93 cells.

Video 1 (WT) and Video 2 (KO) neutrophil migration in Dunn chamber assay.

1. Zhang Y, Tang W, Jones MC, Xu W, Halene S, Wu D. Different roles of G protein subunits beta1 and beta2 in neutrophil function revealed by gene expression silencing in primary mouse neutrophils. *J Biol Chem.* 2010;285(32):24805-24814.

Table S1 Actin Cytoskeletal Genes down-regulated

<b>GENE</b>	<b>LOCUS</b>	<b>KO_FPKM</b>	<b>WT_FPKM</b>	<b>Fold Change WT vs KO</b>	<b>p_value</b>
<b>Hunk</b>	chr16:90386396-90499553	0.0243873	2.68032	109.91	0
<b>Srf</b>	chr17:46546838-46556162	0.43898	13.7479	31.32	0
<b>Lhx1</b>	chr11:84519378-84525534	0.13868	3.77373	27.21	0
<b>Acta1</b>	chr8:123891766-123894736	3.48133	47.4917	13.64	0
<b>Lima1</b>	chr15:99778467-99875456	0.78814	8.92323	11.32	0
<b>Actg1</b>	chr11:120345689-120348484	261.927	2246	8.57	0
<b>Myh11</b>	chr16:14194526-14291408	0.0590963	0.496764	8.41	6.14E-13
<b>Fscn2</b>	chr11:120361533-120368173	0.0447551	0.308896	6.90	0.00101364
<b>Clip2</b>	chr5:134489385-134552434	0.914883	5.98154	6.54	0
<b>Tpm4</b>	chr8:72135291-72153129	42.5116	223.3	5.25	0
<b>Cnn2</b>	chr10:79697304-80369637	113.203	586.467	5.18	0.00118772
<b>Lyst</b>	chr13:13590408-13777440	13.2339	67.3001	5.09	0
<b>Fgd3</b>	chr13:49263109-49309208	19.3645	81.0618	4.19	0
<b>Zyx</b>	chr6:42349827-42358395	85.9583	353.862	4.12	0
<b>Wdr1</b>	chr5:38526812-38561595	62.3782	244.644	3.92	0
<b>Numb</b>	chr12:83795438-83842343	14.4483	54.489	3.77	0
<b>Actb</b>	chr5:142903115-142906724	1268.47	4666.63	3.68	2.22E-16
<b>Myh9</b>	chr15:77760588-77842115	106.398	368.155	3.46	0
<b>Acta2</b>	chr19:34241090-34255336	12.8751	43.505	3.38	0
<b>Diap1</b>	chr18:37844824-37935411	34.2191	113.32	3.31	0
<b>Myh10</b>	chr11:68691914-68816624	0.46816	1.48505	3.17	4.01E-10
<b>Egr1</b>	chr18:34861206-34864956	3.77816	11.7991	3.12	4.91E-14
<b>Coro1a</b>	chr7:126699773-126704754	479.265	1231.28	2.57	2.88E-12
<b>Wasf2</b>	chr4:133130632-133198330	17.2757	43.5538	2.52	7.83E-13
<b>Flna</b>	chrX:74223460-74246534	161.403	403.3	2.50	2.79E-10
<b>Ssh2</b>	chr11:77216424-77460219	18.5403	46.313	2.50	3.86E-13
<b>Tln1</b>	chr4:43531512-43562583	64.2728	149.742	2.33	1.93E-10
<b>Pik3cd</b>	chr4:149649167-149701629	37.7274	87.668	2.32	5.23E-09
<b>Pip5k1a</b>	chr3:95059595-95106858	4.85599	10.7838	2.22	1.93E-07

Table S2: Inflammation Genes down-regulated

<b>GENE</b>	<b>LOCUS</b>	<b>KO_FPKM</b>	<b>WT_FPKM</b>	<b>Fold Change WT vs KO</b>	<b>p_value</b>
<b>Ctse</b>	chr1:131638313-131675507	13.8066	199.429	14.44	0
<b>Nlrp3</b>	chr11:59542685-59566956	7.09473	40.9297	5.77	0
<b>Tlr8</b>	chrX:167242731-167263788	4.1957	22.1173	5.27	0
<b>Lyst</b>	chr13:13590408-13777440	13.2339	67.3001	5.09	0
<b>Cxcr1</b>	chr1:74191785-74194631	1.02741	4.93035	4.80	3.45E-13
<b>Il1b</b>	chr2:129364579-129375733	54.5063	257.206	4.72	0
<b>Nlrp12</b>	chr7:3221509-3249740	10.5163	43.4205	4.13	0
<b>Ccl6</b>	chr11:83582060-83623693	260.361	990.904	3.81	0
<b>Tlr5</b>	chr1:182954787-182976044	4.26425	15.362	3.60	0
<b>Il6ra</b>	chr3:89869323-89913162	16.0212	50.4615	3.15	0
<b>Cxcr2</b>	chr1:74153993-74161246	200.837	596.357	2.97	4.44E-16
<b>Tlr13</b>	chrX:106143274-106160493	31.9984	94.2462	2.95	0
<b>Ccr1</b>	chr9:123962125-123968692	72.049	211.234	2.93	0
<b>Tlr6</b>	chr5:64953094-64960034	4.8346	13.8943	2.87	2.27E-12
<b>Csf3r</b>	chr4:126024658-126044975	247.76	686.976	2.77	4.50E-11



Table S3: Integrin expression

<b>GENE</b>	<b>LOCUS</b>	<b>KO_FPKM</b>	<b>WT_FPKM</b>	<b>Fold Change WT vs KO</b>	<b>p_value</b>
<b>Itga8</b>	chr2:12106659-12312315	0.443401	1.31623	2.97	3.61E-08
<b>Itgal</b>	chr7:127296259-127335137	60.3137	149.629	2.48	1.10E-10
<b>Itgam</b>	chr7:128062639-128118491	417.826	694.321	1.66	0.00484506
<b>Itgb7</b>	chr15:102215994-102231935	26.4388	35.9967	1.36	0.0181999
<b>Itga4</b>	chr2:79255425-79428988	13.8089	16.9807	1.23	0.105993
<b>Itga5</b>	chr15:103344285-103366748	3.45827	3.49268	1.01	0.949019
<b>Itgb3</b>	chr11:104607999-104670471	16.0616	16.0745	1.00	0.99505
<b>Itgb1</b>	chr8:128685653-128733579	23.7798	21.9456	0.92	0.531771
<b>Itgb2l</b>	chr16:96422297-96443614	366.189	273.483	0.75	0.0303399
<b>Itgb2</b>	chr10:77530347-77565674	554.921	979.876	0.62	7.77E-05
<b>Itgad</b>	chr7:128173945-128206366	1.90972	1.03751	0.54	0.00195022
<b>Itga9</b>	chr9:118606708-118901003	0.495038	0.222523	0.45	0.00909608
<b>Itga2</b>	chr13:114835911-114932041	0.24647	0.0917129	0.37	0.00247215
<b>Itga2b</b>	chr11:102453296-102469883	3.0518	1.11977	0.37	3.99E-08

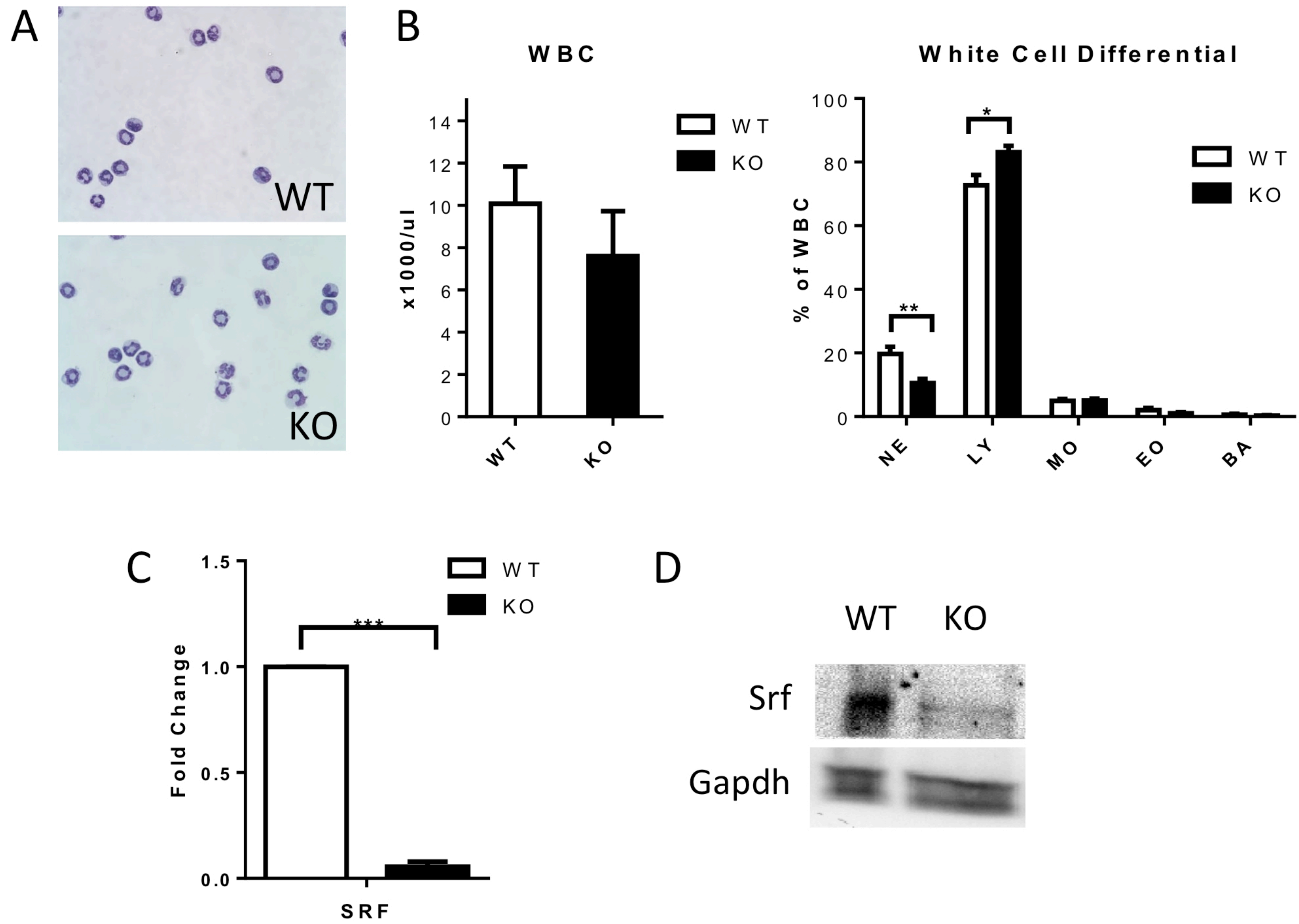


Figure S1



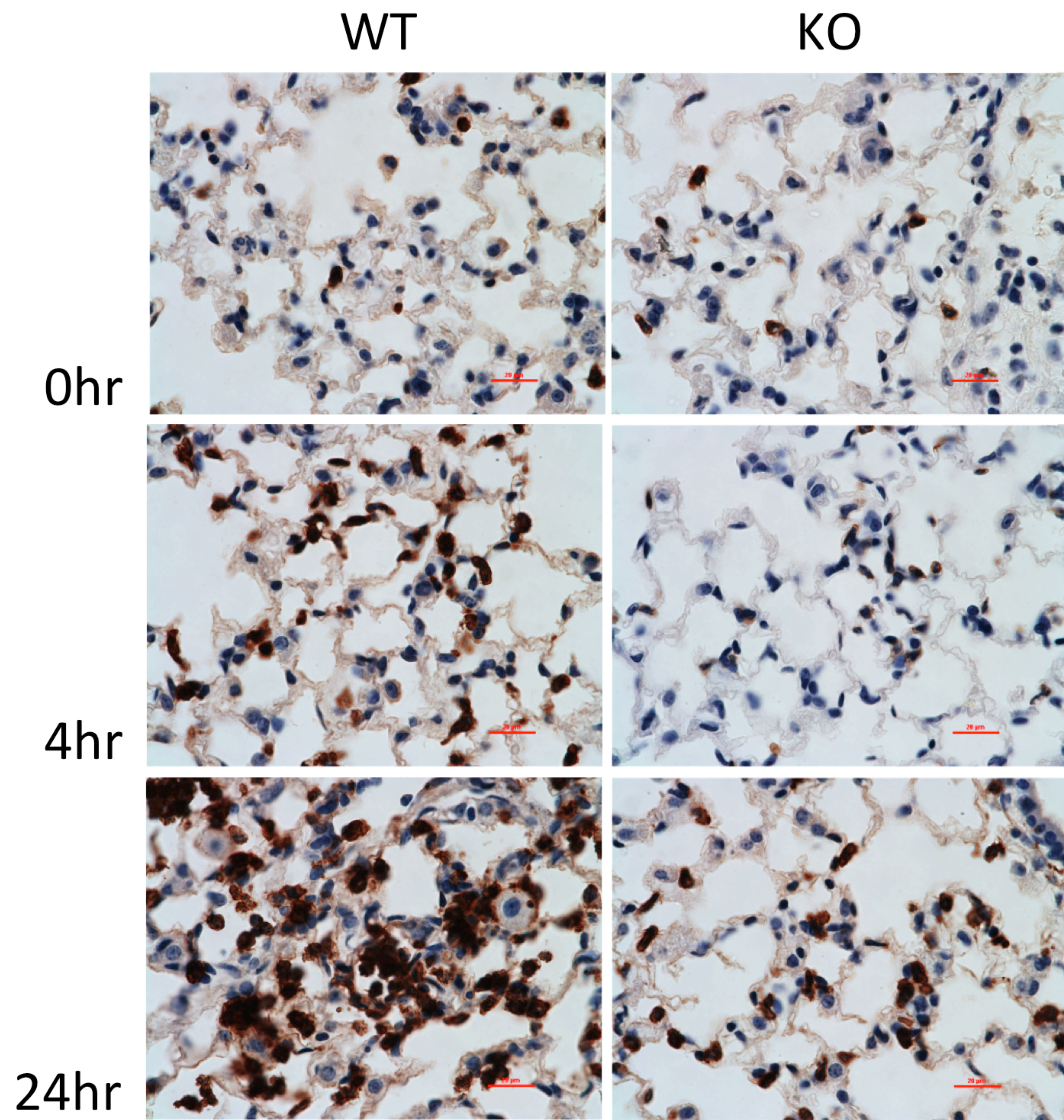


Figure S2



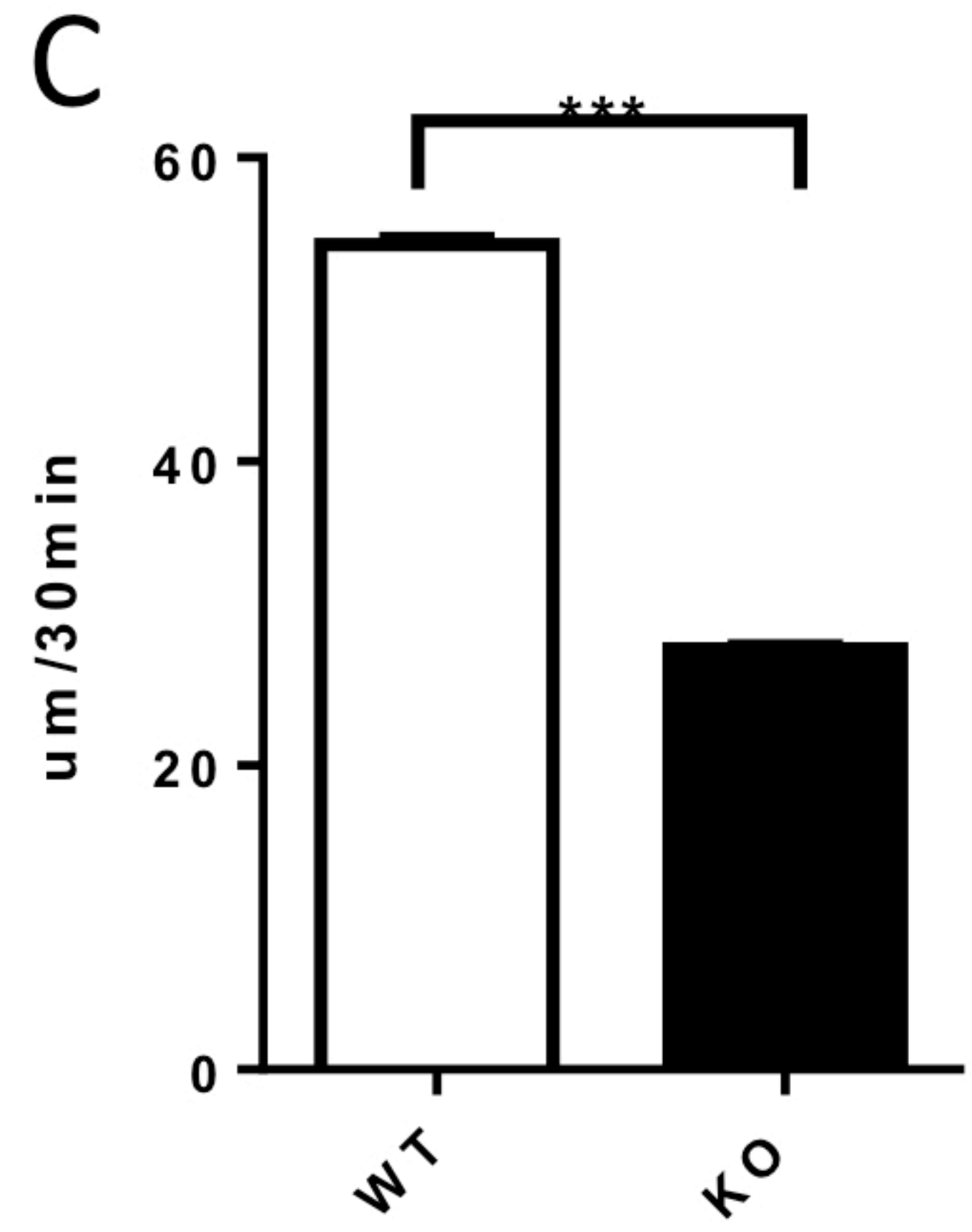
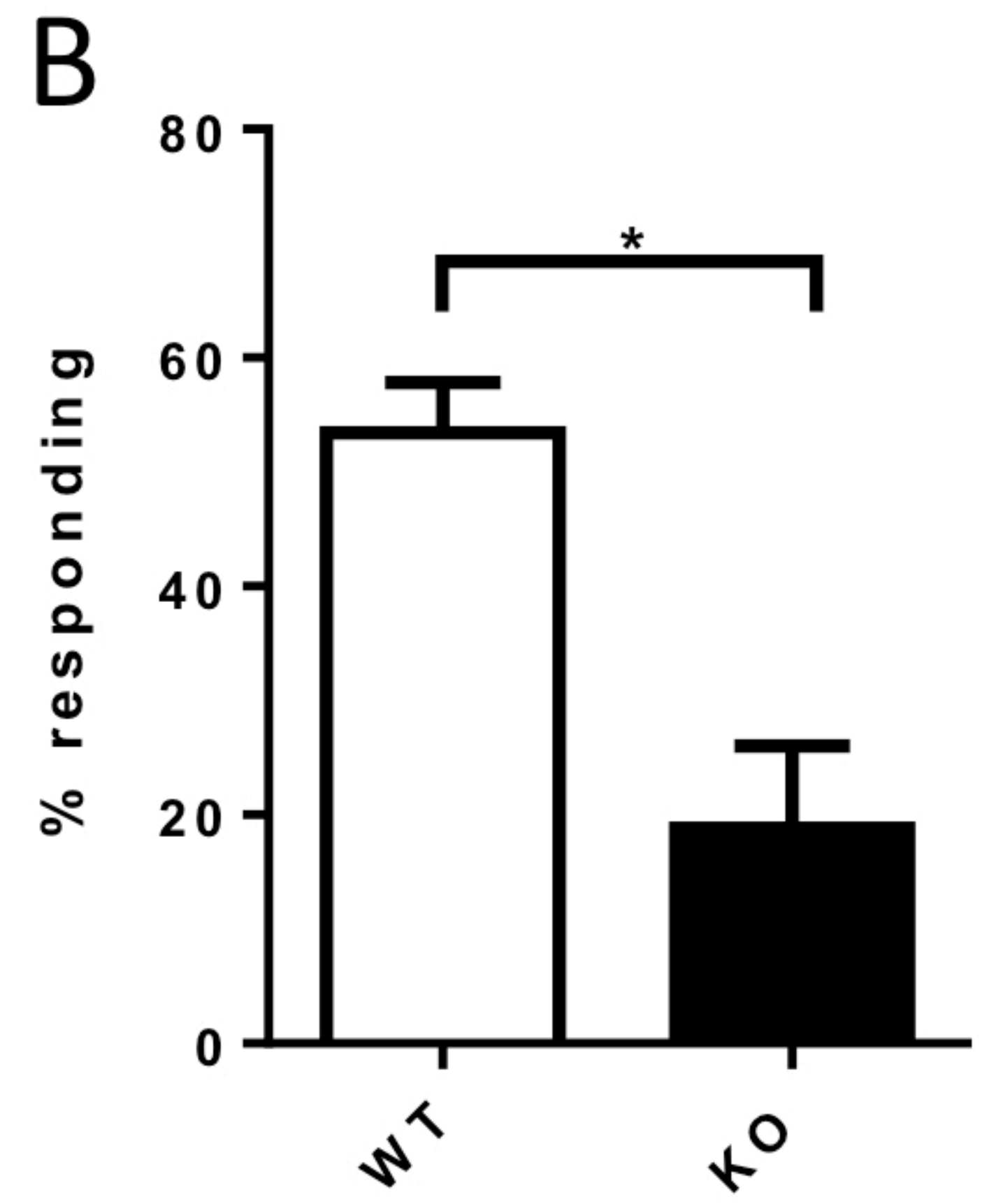
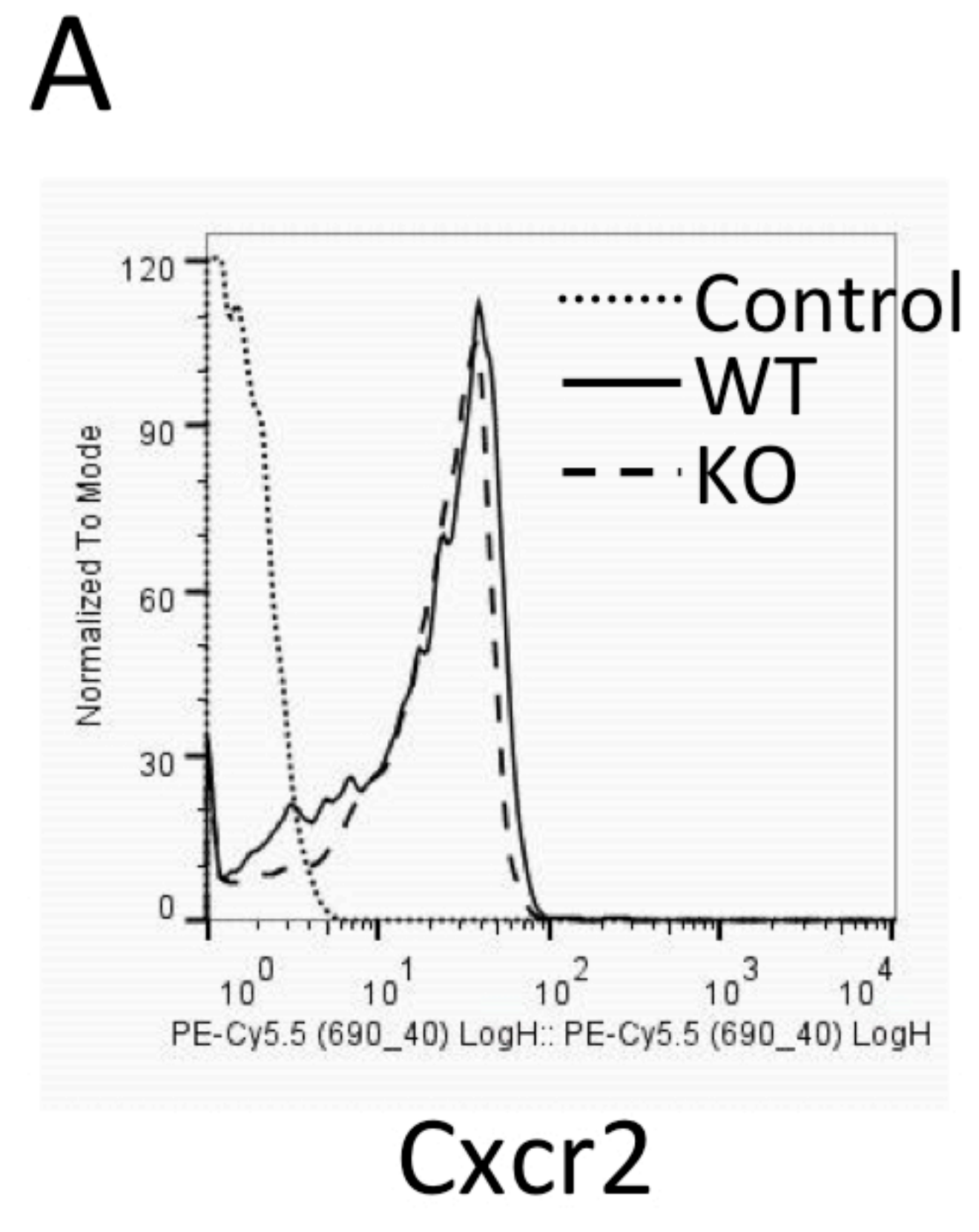


Figure S3

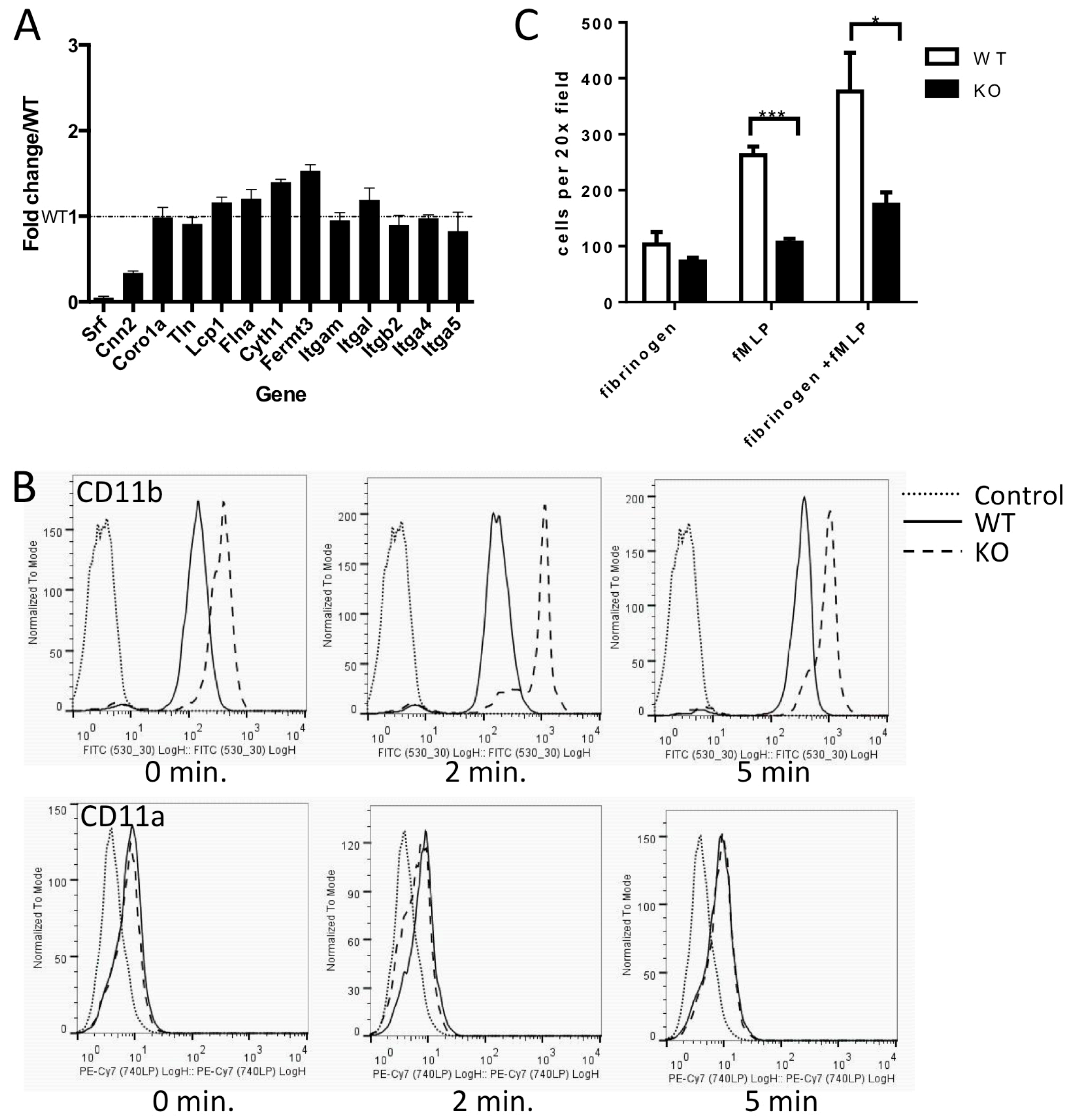


Figure S4



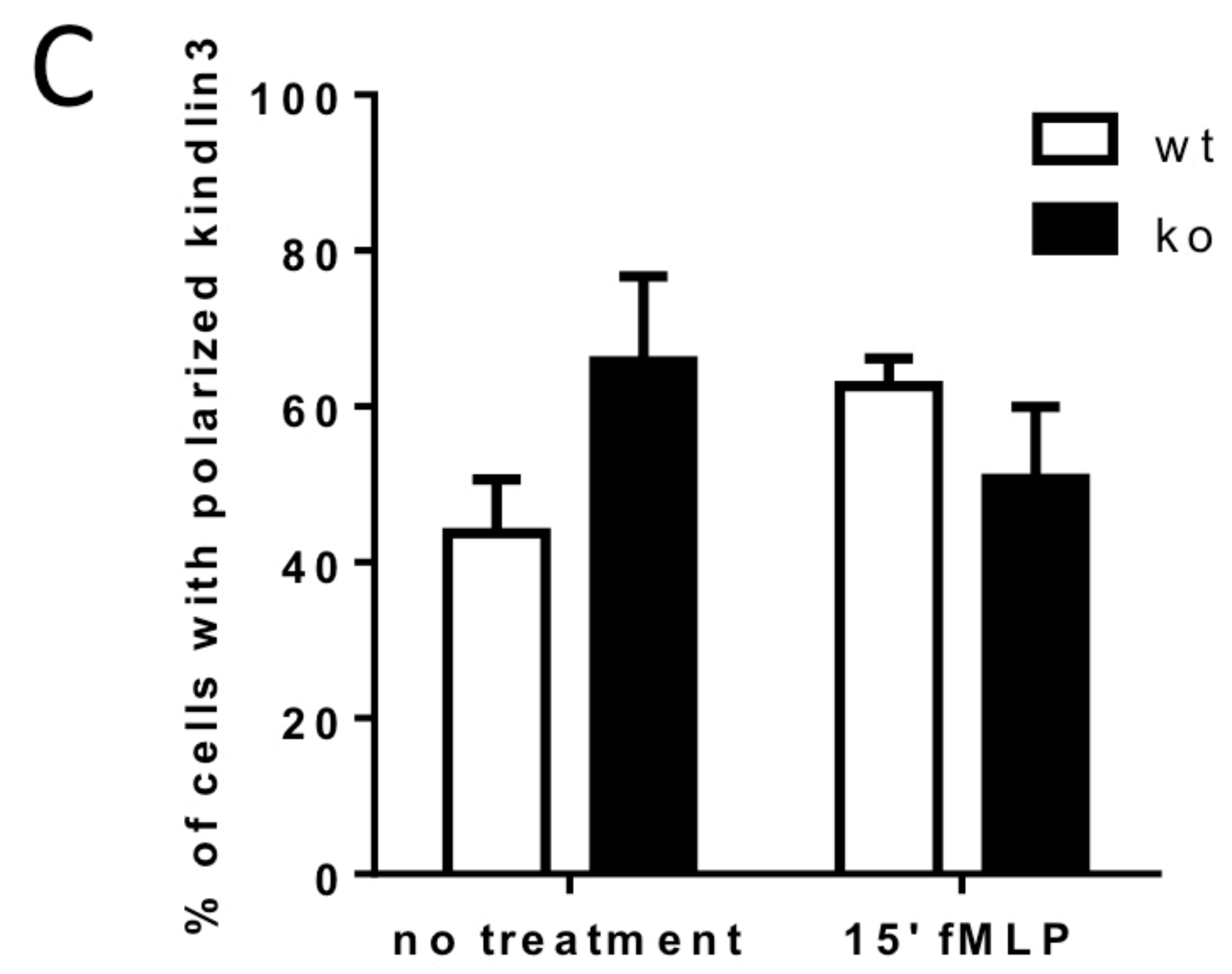
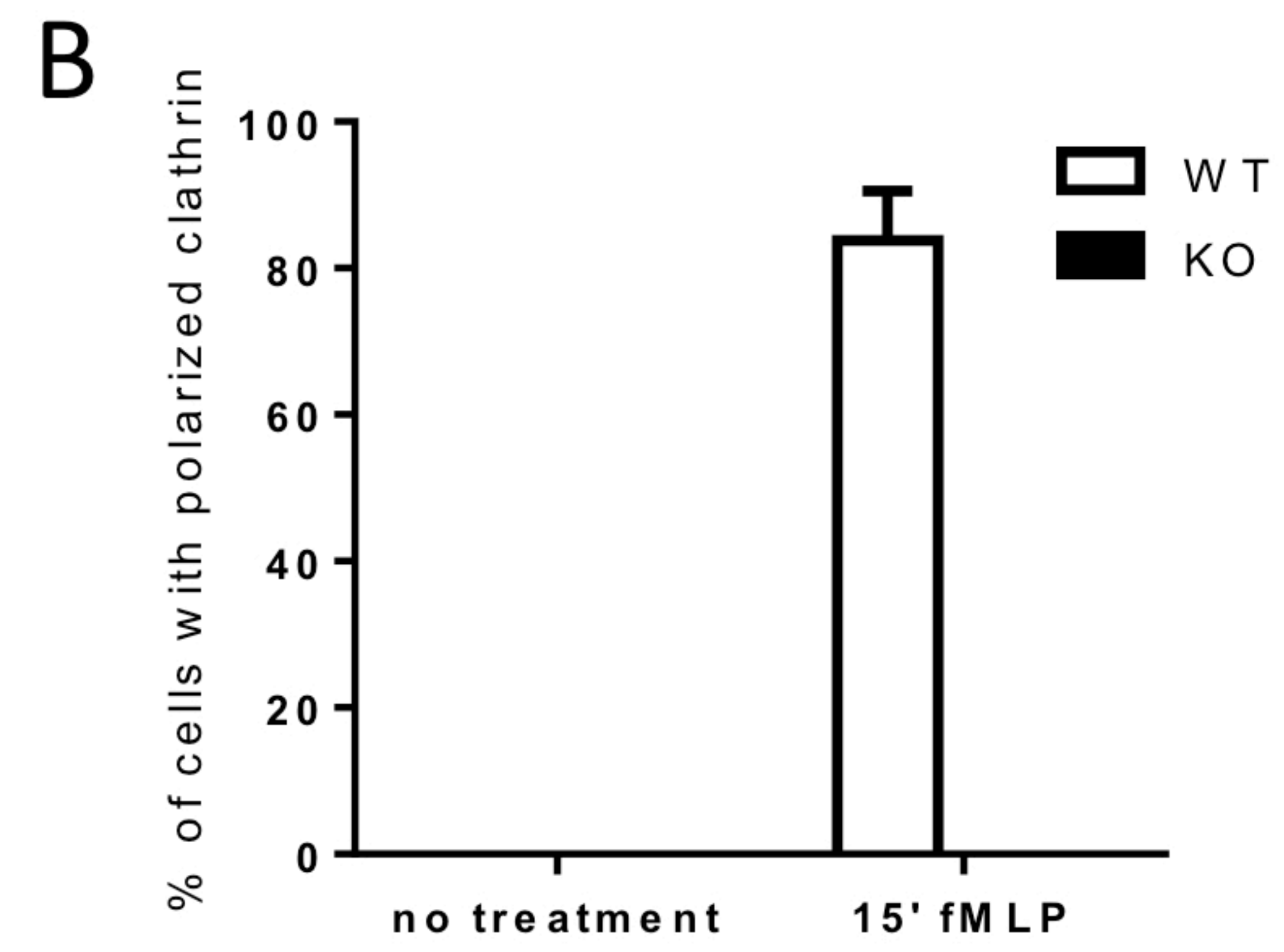
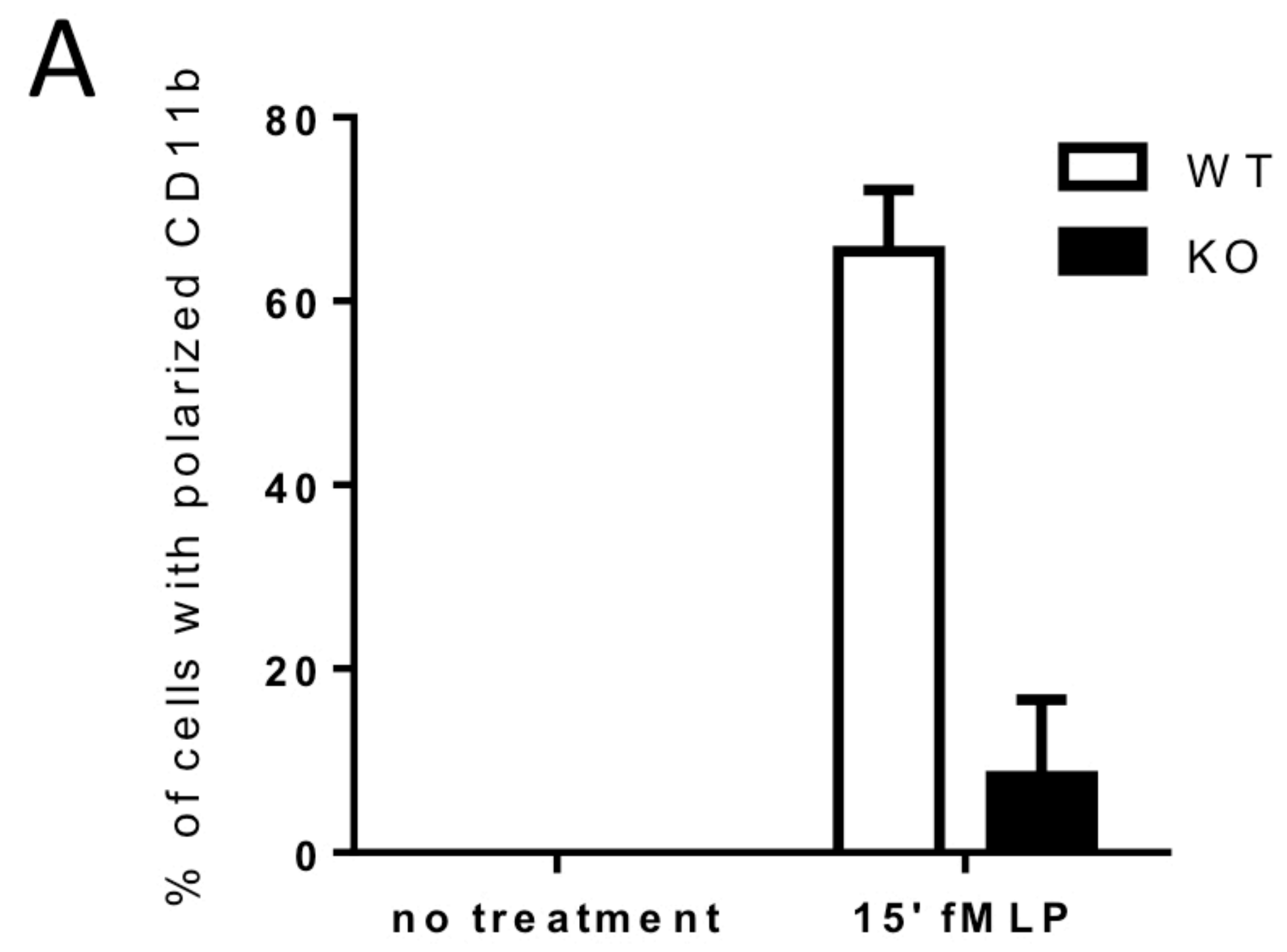


Figure S5